DOI: 10.1002/chem.200600021

Fullerene Polypyridine Ligands: Synthesis, Ruthenium Complexes, and Electrochemical and Photophysical Properties

Zhiguo Zhou,*[a, e] Ginka H. Sarova,[b] Sheng Zhang,[c] Zhongping Ou,[d] Fatma T. Tat,[a] Karl M. Kadish,[d] Luis Echegoyen,[c] Dirk M. Guldi,[b] David I. Schuster,[a] and Stephen R. Wilson*[a, e]

Abstract: Fullerene coordination ligands bearing one bipyridine or terpyridine unit were synthesized, and their coordination to ruthenium(II) formed linear rod-like donor–acceptor systems. Steady-state fluorescence of $[Ru(bpy)_2(bpy\text{-}C_{60})]^{2+}$ showed a rapid solvent-dependent, intramolecular quenching of the ruthenium(II) MLCT excited state. Time-resolved flash photolysis in CH_3CN revealed characteristic transient absorption changes that have been ascribed to the formation of the C_{60} triplet state, suggesting that photoexcitation of $[Ru(bpy)_2(bpy\text{-}C_{60})]^{2+}$ results in a rapid intramolecular transduction of triplet excited state energy. The electrochemical studies on both $[Ru(bpy)_2(bpy\text{-}C_{60})]^{2+}$ and $[Ru(tpy)(tpy\text{-}C_{60})]^{2+}$ indicated electronic coupling between the metal center and the fullerene core.

Keywords: coordination modes · electrochemistry · fullerenes · photochemistry · polypyridine

Introduction

Photoinduced electron transfer (ET) and energy transfer (ENT) in molecular systems combining various donors and fullerene acceptors have been extensively studied, and their electrochemical and photophysical properties are particularly interesting.[1] In recent years, the preparation of various donor–acceptor systems by coordination of fullerene derivatives bearing one pyridine or polypyridine unit to transition metals have been reported in the literature.[2,3] Modulation of the electronic coupling between C_{60} acceptor and various donors is a major goal in the synthetic organic chemistry of fullerenes that may lead to more efficient behavior in charge-transfer processes.[4] In the pursuit of optimal electronic and structural connectors between fullerene cores and photo- and/or electroactive donors, our interest was drawn to *N*-pyridinofulleropyrrolidine compounds. We have previously reported on one such ligand, *N*-pyridyl-3,4-fulleropyrrolidine (**1**).[5] Strong electronic interaction between the fullerene core and metalloporphyrin donors was observed in the study of its axial ligation with a variety of metalloporphyrins, suggesting interesting photochemically induced ET or ENT mechanisms.[5,6]

The synthesis and study of polypyridylruthenium complexes with electron-accepting fullerene cores is particularly interesting from both the photophysical and electrochemical points of view.[3] Several polypyridine ligands, such as 2,2′-bipyridine (bpy), 2,2′:6′,6″-terpyridine (tpy), 1,10-*ortho*-phenanthroline, 3-(2-pyridyl)pyrazoline, 2,3-bipyridine-2-yl-quinoxaline, and 3,6-di(2-pyridyl)pyridazine, have been covalently attached to C_{60} through either flexible or rigid spacers.[3,7] We were interested in the synthesis of the bipyridine and terpyridine variants of compound **1**, in which the bipyridyl

[a] Dr. Z. Zhou, Dr. F. T. Tat, Prof. Dr. D. I. Schuster, Dr. S. R. Wilson
Department of Chemistry, New York University
New York, NY 10003 (USA)
Fax: (+1) 434-483-4195
E-mail: zhouz@lunananoworks.com
wilsons@lunananoworks.com.

[b] Dr. G. H. Sarova, Prof. Dr. D. M. Guldi
Institut für Physikalische und Theoretische Chemie
Universität Erlangen-Nürnberg
Egerlandstr. 3, 91058 Erlangen (Germany)

[c] Dr. S. Zhang, Prof. Dr. L. Echegoyen
Department of Chemistry, Clemson University
Clemson, SC 29634 (USA)

[d] Dr. Z. Ou, Prof. Dr. K. M. Kadish
Department of Chemistry, University of Houston
Houston, TX 77204 (USA)

[e] Dr. Z. Zhou, Dr. S. R. Wilson
Current address: Luna nanoWorks, 521 Bridge Street
Danville, VA 24541 (USA)

Supporting information for this article is available on the WWW under http://www.chemeurj.org/ or from the author. It contains the selected NMR spectra and MALDI-TOF mass spectra of compounds **2**–**8** and CVs of $[Ru(bpy)_2(bpy\text{-}C_{60})][PF_6]_2$ in PhCN and $[Ru(tpy)(tpy\text{-}C_{60})][PF_6]_2$ in CH_3CN/ODCB.

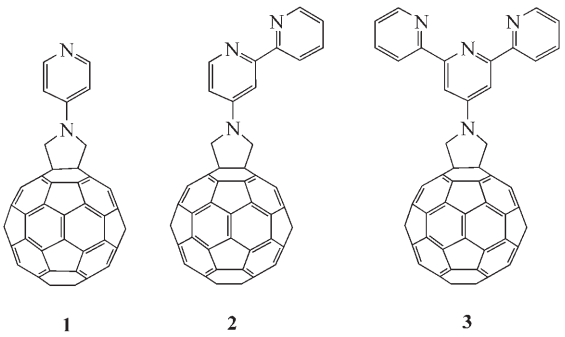

1 2 3

and terpyridyl building blocks were directly attached to the nitrogen atom of the fulleropyrrolidines. Compounds **2** and **3** can serve as bidentate and tridentate ligands, respectively, to coordinate transition metals. The fulleropyrrolidine nitrogen atom has good communication with the fullerene core;[8] therefore we decided to employ a combination of these structural elements for the bridge between the fullerene core and metal centers. We report herein on the synthesis, electrochemistry and photophysics of $[Ru(bpy)_2(bpy\text{-}C_{60})][PF_6]_2$, as well as the synthesis and electrochemical study on $[Ru(tpy)(tpy\text{-}C_{60})][PF_6]_2$.

Results and Discussion

Synthesis of fulleropyrrolidine 2 and its complex $[Ru(bpy)_2(bpy\text{-}C_{60})][PF_6]_2$ (5): To prepare a fulleropyrrolidine **2** with a bipyridyl substituent, the precursor *N*-[4-(2,2′-bipyridyl)]-glycine (**4**) had first to be prepared. As far as we know, this compound has not been reported previously. In our previous study, *N*-pyridylglycine was prepared in a high yield by the treatment of 4-aminopyridine with HCHO, $NaHSO_3$, KCN and HCl.[5] The same treatment of 4-aminobipyridine only afforded **4** in very low yield, mainly due to the insolubility of 4-aminobipyridine in water. Compound **4** was finally synthesized from 4-amino-(2,2′-bipyridine) through reductive amination (H_2, 35 psi, 10% Pd/C) with ethyl glyoxylate[9] in a yield of 82% in the presence of concentrated HCl (Scheme 1). 4-Amino-(2,2′-bipyridine) was prepared in three steps from 2,2′-bipyridine by sequential oxidation, nitration, and catalytic reduction by using slightly modified procedures from the literature.[10] *N*-Bipyridylfulleropyrrolidine (**2**) was then synthesized in 52% yield by azomethine ylide cycloaddition to C_{60} (Scheme 1) and characterized by NMR spectroscopy and MALDI-MS. The coordination of ligand **2** to Ru^{II} was accomplished by refluxing with $[Ru(bpy)_2(Cl)_2]$ in the presence of excess NH_4PF_6 in a mixture of 1,2-dichloroethane (DCE) and orthodichlorobenzene (ODCB). The mixed solvent was necessary to ensure that all starting materials were sufficiently dissolved. The coordination reaction was monitored by TLC, until the disappearance of compound **2**. Complex **5** was very soluble in acetonitrile and reasonably soluble in acetone, benzonitrile, and CH_2Cl_2. Its MALDI mass spectrum shows peaks at $m/z = 1474.6$ and

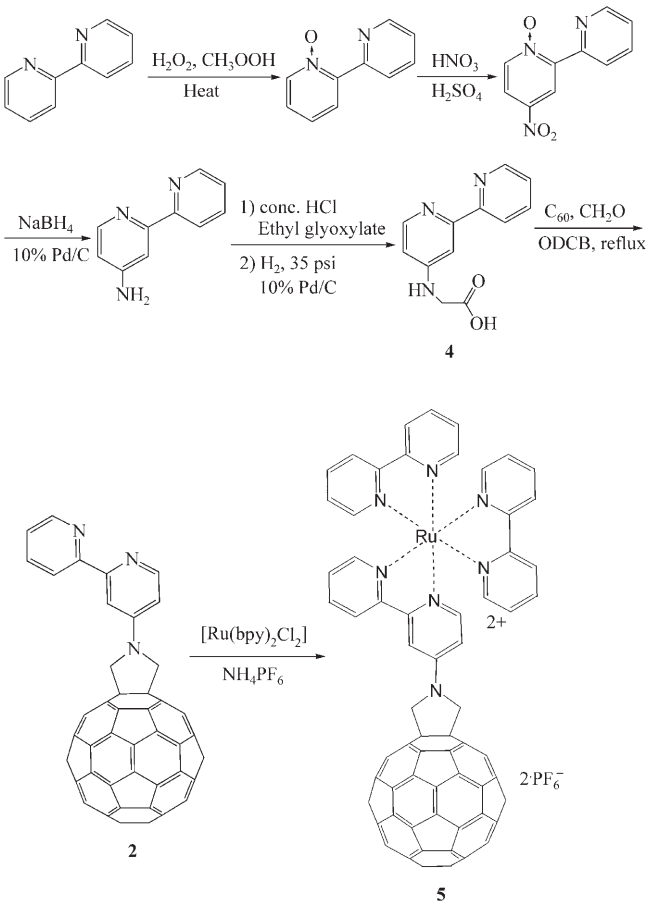

Scheme 1. Synthesis of fulleropyrrolidine **2** and its Ru^{II} complex **5**.

1330.2 corresponding to the loss of one PF_6 and two PF_6 groups, respectively. Interestingly, ions corresponding to addition of oxygen, that is, $[M-2PF_6+O]^+$ and $[M-2PF_6+O_2]^+$ were also observed.

To explore the nature of this unique complex, molecular modeling was performed at the semiempirical AM1 level using Spartan. The complex incorporates a linear metal–fullerene communication pathway through the pyrrolidine nitrogen atom on the basis of the computational study (Figure 1). The bipyridyl unit was directly attached to the nitrogen atom of the pyrrolidine ring to ensure a linear rod-like donor–acceptor structure. A similar configuration was also observed in the study of axial ligation of ligand **1** with Zn–TPP.[5]

Electrochemistry and spectroelectrochemistry of complex 5: The analysis of the cyclic voltammetric behaviour of dyad **5** was obtained in 0.1 M $TBA[PF_6]/CH_2Cl_2$ (TBA = tetrabutylammonium) at the glassy carbon electrode (GCE). The CVs of ligand **2**, complex **5**, and reference compound $[Ru(bpy)_3]^{2+}$ in the cathodic region are shown in Figure 2. From the comparison of the redox potentials of complex **5** with those of ligand **2** and the reference compound, the reductions with $E_{1/2}$ values of −1.03, −1.39, and −1.92 V were assigned to C_{60}-centered one-electron reversible reduction

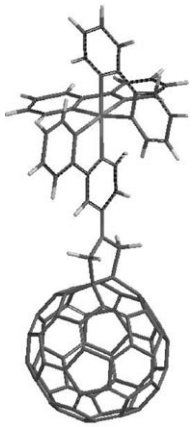

Figure 1. Spartan model of complex **5**.

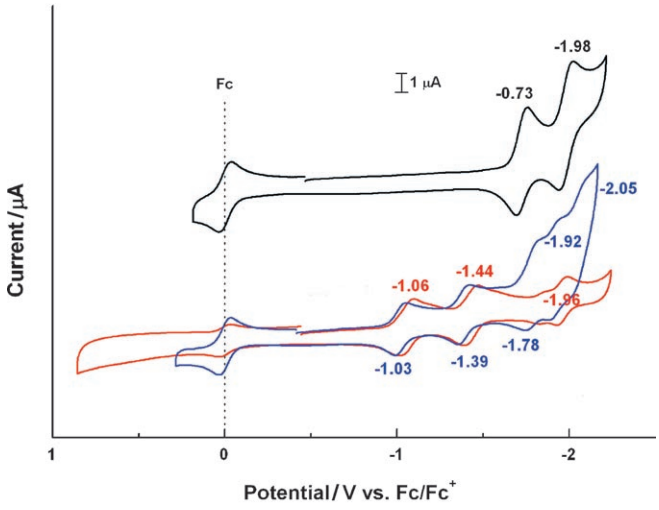

Figure 2. Cyclic Voltammograms of $[Ru(bpy)_3]Cl_2$ (black), bpy-C_{60} (red) and complex **5** (blue) in CH_2Cl_2 with 0.1 M $TBA[PF_6]$.

processes, and the reduction located at −1.78 V was assigned to the first reduction of the $[Ru(bpy)_3]^{2+}$ unit. The reduction potentials of the fullerene moiety shifted positively by 30–50 mV from ligand **2** to complex **5**, suggesting that reduction of the fullerene unit in complex **5** is easier than that in the free ligand **2**. On the other hand, the Ru-based reduction potentials of the complex **5** shifted negatively by 50 mV relative to those of the reference compound $[Ru(bpy)_3]Cl_2$, suggesting that the reduction of ruthenium metal center becomes more difficult in the complex. Similar electrochemical results were also obtained in PhCN (see Supporting Information). The first Ru-based oxidation potential of complex **5** is negatively shifted by 140 mV relative to that of $[Ru(bpy)_3]Cl_2$ in PhCN, and this negative oxidation potential shift was 250 mV in CH_2Cl_2 (Table 1). This half-wave potential change (compared to the small C_{60}-centered reduction potential changes, that is, 30–50 mV) can be explained by the electron-donating effect of the amino substituent on one bpy unit in dyad **5**.

Table 1. $E_{1/2}$ [V vs. Fc/Fc^+] values for the bpy series in CH_2Cl_2 and for tpy series in ODCB/CH_3CN (4:1) with 0.1 M $TBAPF_6$.

	Oxidation	Reduction				
		I	II	III	IV	V
C_{60}-bpy		−1.06	−1.44	−1.96		
$[Ru(bpy)_2(bpy\text{-}C_{60})]^{2+}$	0.69	−1.03	−1.39	−1.78	−1.92	−2.05
$[Ru(bpy)_3]^{2+}$	0.94	−1.73	−1.98			
C_{60}-tpy		−1.07	−1.46	−1.99		
$[Ru(tpy)(tpy\text{-}C_{60})]^{2+}$	0.59	−1.04	−1.43	−1.76	−2.02	
$[Ru(tpy)_2]^{2+}$	0.86	−1.66	−1.96			
$[Ru(tpy)(tpy\text{-}NH_2)]^{2+}$	0.58	−1.75				

Thin-layer UV/Vis spectroelectrochemistry was carried out in CH_2Cl_2 containing 0.2 M $TBA[PF_6]$. The spectral changes of complex **5** obtained upon the first reduction and first oxidation in CH_2Cl_2 are illustrated in Figure 3. A spectrum with maxima at 770 and 995 nm was obtained upon the

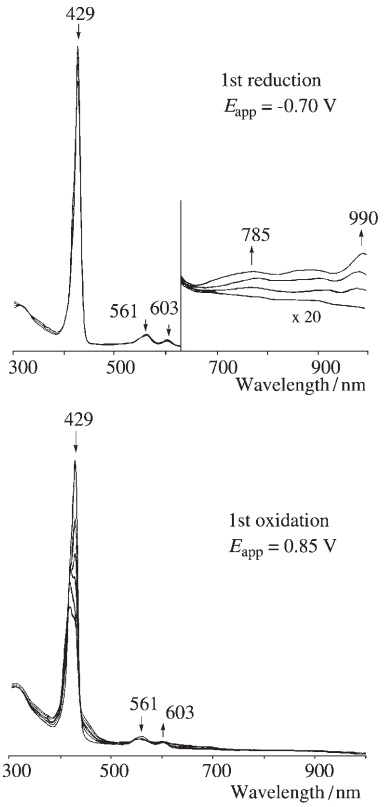

Figure 3. Thin-layer UV/Vis spectral changes of complex **5** during the first reduction (top) and the first oxidation (bottom) in CH_2Cl_2 containing 0.2 M $TBA[PF_6]$.

first controlled-potential reduction at −0.70 V. The absorption band around 1000 nm is known to be a diagnostic marker of monofunctionalized fullerene radical anion.[11] The spectral changes obtained upon the electrochemical oxidation of complex **5** at an applied potential of 1.40 V were almost identical to that of $[Ru(bpy)_3]Cl_2$ obtained under the same experimental conditions, and indicated that the first oxidation of complex **5** occurred at the ruthenium metal center.

Absorption spectra: The ground-state absorption spectra of complex **5**, ligand **2**, and reference compound $[Ru(bpy)_3]Cl_2$ were recorded in CH_2Cl_2 (Figure 4). Complex **5** shows the typical absorption bands of both the fullerene ligand and

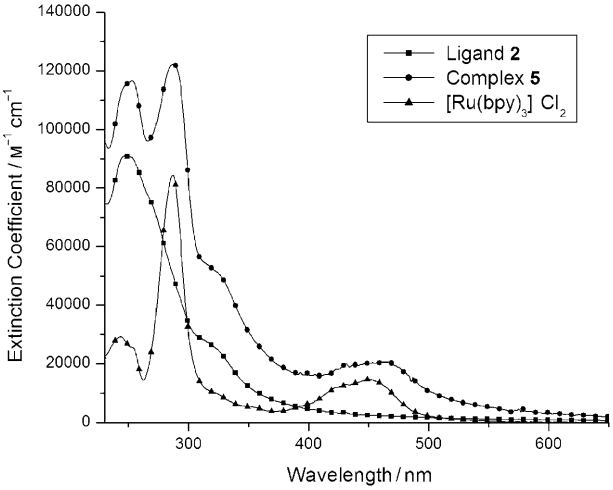

Figure 4. Absorption spectra of ligand **2**, complex **5** and $[Ru(bpy)_3]Cl_2$ in CH_2Cl_2.

the reference compound, namely the monofunctionalized fulleropyrrolidine band at 430 nm and the metal-to-ligand charge transfer (MLCT) transition band of the trisbipyridyl ruthenium complex at 400–500 nm. The MLCT absorption of dyad **5** is subjected to a red-shift relative to the reference compound $[Ru(bpy)_3]^{2+}$. In line with the electrochemical results, these data suggest there is electronic coupling existing between the fullerene core and the ruthenium metal center.

Luminescence spectra and time-resolved photolysis: To investigate the extent of electronic interaction between the MLCT excited state and the fullerene ground state, steady state and time-resolved emission measurements were carried out with dyad **5** in solvents of different polarity, and compared to that of reference compound $[Ru(bpy)_3]Cl_2$. Considering the nature of the ruthenium MLCT excited states, namely, triplet character and lifetimes that are on the order of hundreds of nanoseconds, the presence of molecular oxygen plays an indispensable role. In particular, it quenches the MLCT excited state through singlet oxygen formation. Consequently, it was necessary to conduct all emission and transient absorption experiments in oxygen-free solutions. We tested $[Ru(bpy)_3]Cl_2$ in acetonitrile and complex **5** in dichloromethane, dichloromethane/acetonitrile, and acetonitrile by monitoring the characteristically broad and intense MLCT emission that centers around 610 nm. The emission spectra were taken for solutions with equal absorbance at the 456 nm excitation wavelength. Relative to $[Ru(bpy)_3]^{2+}$, we noticed a strong quenching of the emission intensity for the cation of complex **5** (Figure 5). Interestingly, the extent of emission quenching increases with solvent polarity, and the relative intensities are 0.14 in dichloromethane, 0.1 in dichloromethane/acetonitrile, and 0.07 in acetonitrile; the emission intensity of $[Ru(bpy)_3]^{2+}$ in acetonitrile was set arbitrarily as 1. This trend infers highly efficient electronic couplings between the donor and acceptor components. A similar trend evolves when looking at the time-resolved emission decays. For $[Ru(bpy)_3]^{2+}$ in acetonitrile, a lifetime of 565 ns is seen, while a lifetime of 0.31 ns was derived for complex **5**.

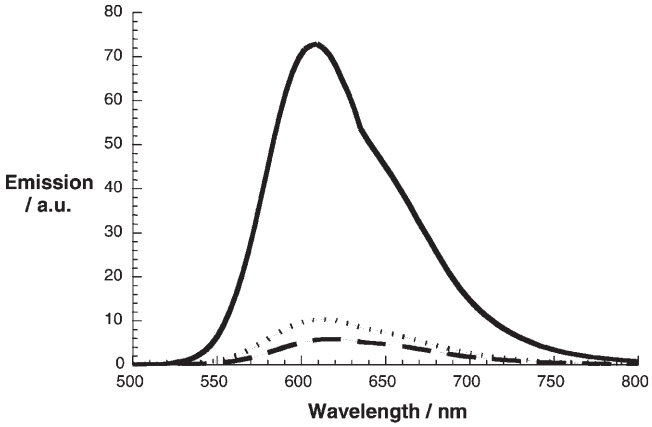

Figure 5. Room temperature emission spectra of $[Ru(bpy)_3]Cl_2$ in deoxygenated acetonitrile (solid line) and complex **5** in deoxygenated CH_2Cl_2 (dotted line) and deoxygenated CH_3CN (dashed line) with matching absorption at the 456 nm.

Steady-state and time-resolved emission experiments reveal unmistakable evidence for pronounced quenching of the MLCT excited-state emission. A product assignment is, however, only possible through complementary transient absorption measurements. We then investigated $[Ru(bpy)_3]^{2+}$ and $[Ru(bpy)_2(bpy\text{-}C_{60})]^{2+}$ upon 387 nm excitation with 150 fs laser pulses. This is expected to form the MLCT excited state almost exclusively, while ligand-centered π–π^* states are not involved at all and fullerene-centered excited states are formed only as a minor product (i.e., less than 5%). For $[Ru(bpy)_3]^{2+}$ we noted a transient absorption spectrum, which on the 1.5 ns scale did not give rise to any appreciable decay (Figure 6). Features of the transient absorption spectrum include strong bleaching of the MLCT transition in the range between 400 and 470 nm and a broad spectrum in the red part of the recorded spectrum. In fact, turning to nanosecond spectroscopy reveals that the MLCT excited-state decays, similar to the conclusion of the time-resolved emission experiments, back to the ground state with unimolecular kinetics. From the decay profiles an MLCT excited-state lifetime of around 350 ns has previously been determined.[3e]

When photoexciting complex **5** in acetonitrile, the spectral characteristics at early times (i.e., immediately following the 150 fs laser pulse) are essentially identical to what has been seen for $[Ru(bpy)_3]^{2+}$. The only notable difference is a slight red shift (Figure 6). These observations affirm the successful MLCT excited-state formation despite the presence of the fullerene. The transient absorptions are, however, unstable on the 1.5 ns timescale. In particular, a rapid decay is dis-

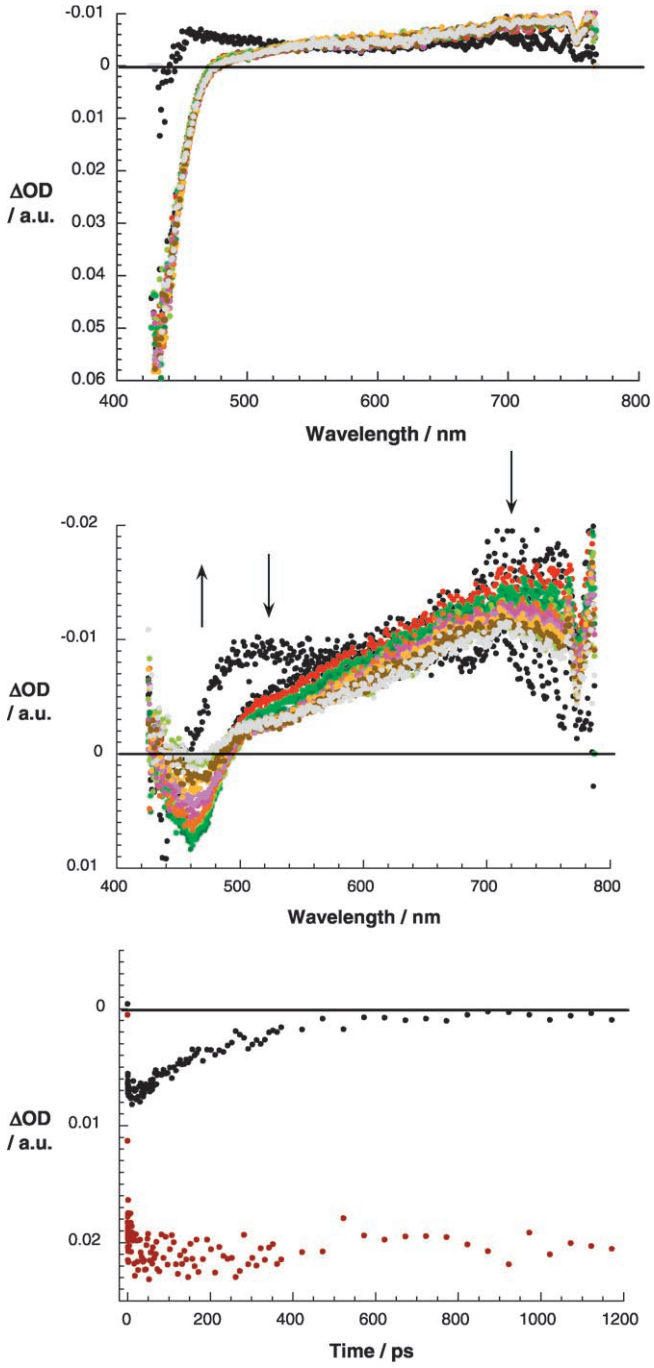

Figure 6. Top: Differential absorption spectra (visible) obtained upon femtosecond flash photolysis (387 nm) of $[Ru(bpy)_3]Cl_2$ (5.0×10^{-6} M) in CH_3CN with several time delays between 0 and 1500 ps at room temperature. Middle: Differential absorption spectra (visible) obtained upon femtosecond flash photolysis (387 nm) of complex **5** (5.0×10^{-6} M) in CH_3CN with several time delays between 0 and 1500 ps at room temperature. Bottom: Time-absorption profiles of $[Ru(bpy)_3]Cl_2$ (red) and complex **5** (black) at 450 nm.

cernable, from which a much shorter MLCT excited-state lifetime of 0.27 ns in acetonitrile was derived. At the conclusion of the intramolecular MLCT excited-state decay, spectral changes evolve that are reminiscent of the fullerene triplet excited state—a broad transient with a maximum at 700 nm—suggesting a rapid intramolecular transduction of triplet excited state energy as shown in Equation (1).

$$[(bpy)_2\text{-Ru-}(bpy\text{-}C_{60})]^{2+} \rightarrow [(bpy)_2\text{-}^{3*}\text{Ru-}(bpy\text{-}C_{60})]^{2+} \rightarrow [(bpy)_2\text{-Ru-}(bpy\text{-}^{3*}C_{60})]^{2+} \quad (1)$$

Such a decay mechanism finds further support upon considering the redox potentials for 1) reducing the electron-accepting fullerene and 2) oxidizing the electron-donating $[Ru(bpy)_3]^{2+}$ complex. The energy of the radical ion pair state is determined as 1.64 eV, which is noticeably higher than that of the fullerene triplet excited state (1.5 eV).[3g] Since triplet-excited-state energy transfer and charge separation both involve electron transfer, the smaller energy gap for the former process (i.e., 0.36 eV)—relative to the latter one (i.e., 0.5 eV)—governs the photoreactivity of complex **5**.

Synthesis of fulleropyrrolidine 3 and $[Ru(tpy)(tpy\text{-}C_{60})][PF_6]_2$ (8): *N*-terpyridyl-3,4-fulleropyrrolidine (**3**) and its complex $[Ru(tpy)(tpy\text{-}C_{60})][PF_6]_2$ (**8**) were synthesized and we expected the electronic coupling between the fullerene core and pyridyl nitrogen atoms to be the same as that in the case of pyridinofullerene ligands **1** and **2**. Ligand **3** is an important intermediate compound in our ongoing studies. Herein, we report the synthesis, characterization and electrochemical behaviour of compound **3** and **8**. In a manner similar to *N*-bipyridyl-3,4-fulleropyrrolidine (**2**), compound **3** was synthesized by [3+2] cycloaddition of the azomethine ylide derived from formaldehyde and *N*-terpyridylglycine (**7**), which was prepared from 4′-aminoterpyridine (**6**) by reductive amination with ethyl glyoxylate[9] in the presence of conc. HCl (Scheme 2). The characterization of compound **7** was established on the basis of MALDI-MS, and ^1H, ^{13}C, and COSY NMR spectroscopy. 4′-Aminoterpyridine was synthesized from commercially available 4′-chloroterpyridine in three steps. 4′-Chloroterpyridine was refluxed with excess hydrazine in isobutanol to form 4′-hydrazinoterpyridine, which was subsequently transformed to 4′-azidoterpyridine in almost quantitative yield.[12] Reaction of 4′-azidoterpyridine with hydrogen sulfide at 0 °C in a mixed solvent of methanol and dichloromethane yielded 4′-aminoterpyridine. Complex **8** was prepared using similar procedures reported previously.[3f] Both ligand **3** and complex **8** were characterized by NMR spectroscopy and MALDI-MS. The mass spectrum of complex **8** shows peaks corresponding to the loss of two, one, and zero PF_6^- counterions.

Electrochemistry of $[Ru(tpy)(tpy\text{-}C_{60})][PF_6]_2$ (8): The cyclic voltammetric behaviour of complex **8** was measured in 1,2-dichlorobenzene/CH_3CN (4:1). The $E_{1/2}$ values of ligand **3**, complex **8**, and reference compounds $[Ru(tpy)_2][PF_6]_2$[13] and $[Ru(tpy)(tpy\text{-}NH_2)][PF_6]_2$[13] are summarized in Table 1. From the CV response of complex **8**, one oxidation and four reduction processes were recorded. The first two reversible waves at −1.04 and −1.43 V versus Fc/Fc^+ correspond to the first and second reduction processes of C_{60}. The third re-

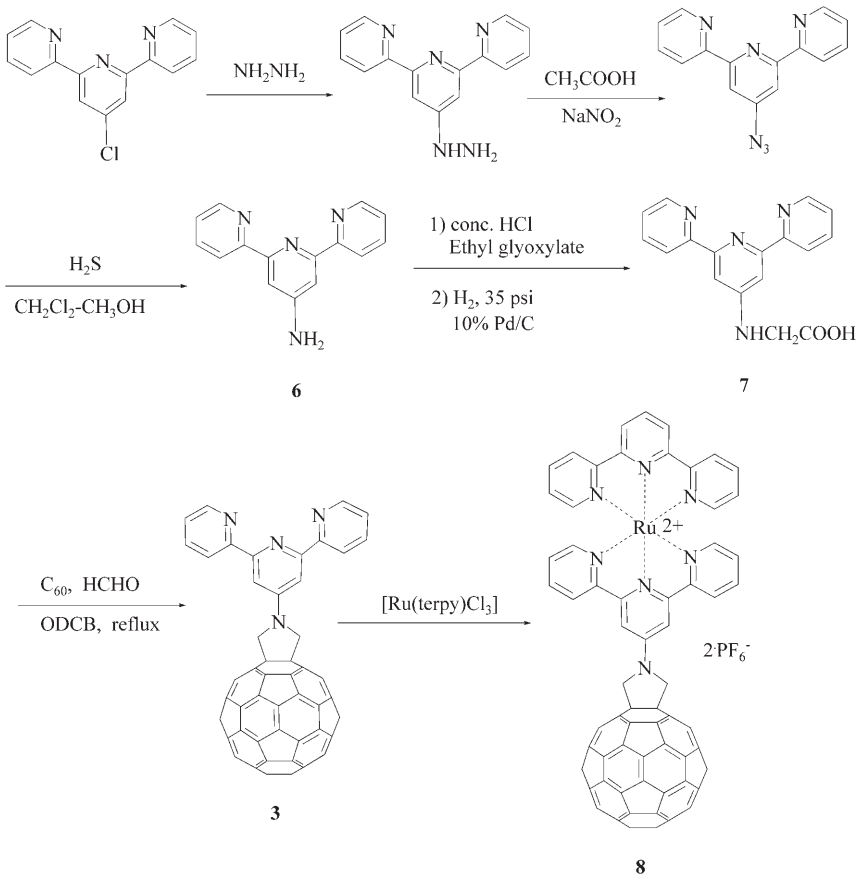

Scheme 2. Synthesis of fulleropyrrolidine ligand **3** and its Ru^{II} complex **8**.

duction at −1.76 V is quasireversible and is assigned to the first reduction of the metal center. The fourth reduction at −2.02 V is broad, which is probably due to the combination of the third reduction of C_{60} and the second reduction of the ruthenium metal center. Compared to those of compound **3**, the first two reductions of compound **8** are anodically shifted by 30 mV, which indicates electronic coupling between C_{60} and the terpyridyl nitrogen atoms. Similar anodical shifts of C_{60}-based reduction potentials were also obtained in the case of *N*-bipyridylfulleropyrrolidine and *N*-pyridylfulleropyrrolidine.[5] The first ruthenium-based reduction of complex **8** is negatively shifted by 100 mV and the first oxidation potential is negatively shifted by 270 mV, relative to $[Ru(tpy)_2]^{2+}$, which are much bigger than those shifts for C_{60}-centered reductions. This could be due to the existence of the amino substituent on one tpy residue in complex **8**.

Conclusion

In this paper, we have described the synthesis, electrochemistry and photophysical behaviour of $[Ru(bpy)_2(bpy\text{-}C_{60})]^{2+}$ and/or $[Ru(tpy)(tpy\text{-}C_{60})]^{2+}$ complexes, in which one bpy or tpy unit was directly attached to the nitrogen atom of a fulleropyrrolidine to ensure a linear communication pathway between the two components. Our studies on the whole series of three *N*-pyridinofulleropyrrolidines **1**--**3** reveal that they are a new type of fullerene ligand with unique electronic properties. In particular, the existence of electronic coupling between the polypyridyl nitrogen atom and fullerene core makes them potential candidates of building blocks for molecular electronics, such as molecular wires and transistors. In this light, pyridyl or polypyridyl fulleropyrrolidine multiple adducts with defined geometry between pyridyl ligation sites need to be properly designed and synthesized. Coordination-driven self-assembly of these fullerene–polypyridyl building blocks may lead to novel supramolecular architectures with interesting electronic properties.[14]

Experimental Section

General: Reagents were purchased from commercial suppliers and used without further purification. NMR spectra were obtained on a Bruker AVANCE-400 or AVANCE-500 NMR spectrometer. The mass spectra were obtained by using a Bruker Omni Flex MALDI-TOF. Fluorescence was monitored by using a Shimadzu RF-5301 spectrophotometer, and absorption spectra were measured on a Perkin-Elmer spectrophotometer.

Electrochemical measurements: All electrochemical measurements were performed in redistilled solvents (degassed with Ar) with 0.1 M TBA[PF_6] as the supporting electrolyte on a CHI 660 Electrochemical Workstation (CH Instruments Inc, Austin, Texas). A platinum wire was employed as the counter electrode. A silver wire was used as the reference. Ferrocene (Fc) was added as an internal reference and all the potentials were referenced relative to the Fc/Fc^+ couple. A glassy carbon electrode (CHI, 3 mm in diameter), polished with 0.3 μm aluminum paste and ultrasonicated in deionized water and CH_2Cl_2 bath, was used as the working electrode. UV/Vis spectroelectrochemical experiments were performed with a home-built thin-layer cell, which had a light transparent platinum-net working electrode. Potentials were applied and monitored with an EG&G PAR Model 173 potentiostat. Time-resolved UV/Vis spectra were recorded with a Hewlett–Packard Model 8453 diode array spectrophotometer.

Photophysical measurements: Femtosecond transient absorption studies were performed with 387 nm laser pulses (1 kHz, 150 fs pulse width) from an amplified Ti:Sapphire laser system (CPA 2101, Clark-MXR). Nanosecond laser flash photolysis experiments were performed with 337 nm laser pulses from a nitrogen laser (8 ns pulse width) in a front face excitation geometry. Fluorescence lifetimes were measured with a Laser Strope Fluorescence Lifetime Spectrometer (Photon Technology International) with 337 nm laser pulses from a nitrogen laser fiber-coupled to a lens-based T-formal sample compartment equipped with a stroboscopic detector. Details of the Laser Strobe systems are described on the manufacture's web site. Emission spectra were recorded with a SLM

8100 spectrofluorometer. The experiments were performed at room temperature. Each spectrum represents an average of at least five individual scans, and appropriate corrections were applied whenever necessary.

Synthesis of 4-amino-2,2′-bipyridine: A mixture of 4-nitro-2,2′-bipyridine-*N*-oxide (1.1 g, 5.1 mmol) in methanol (20 mL) and 10% Pd/C (0.23 g) was cooled in an ice bath and vigorously stirred under an inert atmosphere. Powder sodium borohydride (2.5 g) was added in small portions. Stirring and cooling was continued until gas evolution ceased, and the dissolution of suspended reactant was complete during the course of the reaction. The catalyst was removed by filtration and methanol was evaporated under reduced pressure. Water (60 mL) was added and the aqueous solution was thoroughly extracted with five portions of diethyl ether (50 mL). The combined organic extracts were dried over Na_2SO_4 and evaporated to yield white solid (0.86 g, 95%). ^{1}H NMR (300 MHz, $CDCl_3$): $\delta = 4.56$ (br, 2H; -NH_2), 6.52 (dd, $J = 5.4$, 2.4 Hz, 1H), 7.35 (ddd, $J = 7.7$, 4.8, 1.2 Hz, 1H), 7.66 (d, $J = 2.4$ Hz, 1H), 7.80 (ddd, $J = 8.0$, 7.7, 1.8 Hz, 1H), 8.27 (d, $J = 5.4$ Hz, 1H), 8.35 (d, $J = 8.0$ Hz, 1H), 8.64 ppm (d, $J = 6.4$ Hz, 1H); ^{13}C NMR (75 MHz, $CDCl_3$): $\delta = 107.1$, 109.7, 121.3, 123.5, 136.8, 149.0, 150.0, 153.9, 156.7, 157.0 ppm; ESI-MS: *m*/*z*: 174.1 $[M+H]^+$.

Synthesis of *N*-bipyridyl glycine (4): A solution of 4′-amino-2,2′-bipyridine (1.9 g, 12 mmol), ethyl glyoxylate (50% in toluene, 2.4 g, 12 mmol), water (6 mL), and concentrated HCl (7 mL) were allowed to stand at 25°C for 1 h in a hydrogenation bottle. Catalyst (100 mg of 10% Pd on carbon) was added, and the mixture was hydrogenated on a low-pressure reaction apparatus charged initially at 35 psi until no further absorption of hydrogen was evident (5 h). Water (25 mL) was added, and the mixture was heated on a water bath to dissolve any white precipitate formed during the reaction. Removal of the catalyst by filtration of the warm mixture and evaporation of the filtrate gave the glycine hydrochloride as white solid. Concentrated HCl was added, and the residue was heated at 60°C for 20 mins and then cooled to 0°C. Collection of the solid by vacuum filtration gave (1.52 g, yield 80%) of tan powder in its HCl salt form. The HCl salt was treated with stoichiometric NaOH solid to give compound **4**. ^{1}H NMR (HCl salt; 400 MHz, D_2O): $\delta = 8.63$ (d, $J = 6.7$ Hz, 1H), 8.11–8.24 (m, 2H), 7.89 (m, 2H), 7.30–7.49 (m, 2H), 6.62 (d, $J =$ 5.6 Hz, 2H), 3.80 ppm (s, 2H); MS (MALDI): *m*/*z*: 230 $[M+1]^+$.

Synthesis of *N*-[4-(2,2′-bipyridyl)]fulleropyrrolidine (2): A mixture of C_{60} (100 mg, 0.14 mmol), paraformaldehyde (21 mg, 0.7 mmol), and *N*-bipyridylglycine (62 mg, 0.28 mmol) was heated at reflux in *o*-dichlorobenzene (10 mL) under N_2 for 5 h. The solution was washed with NaCl aqueous solution and dried over Na_2SO_4. The solvent was removed under reduced pressure. The crude product was purified by flash column chromatography on silica (eluant: toluene, then toluene/triethylamine 100:2), affording fulleropyrrolidine **2** (49 mg, 52%). ^{1}H NMR (300 MHz, CS_2/$CHCl_3$, 2/3): $\delta = 5.50$ (s, 4H), 7.06 (dd, $J = 5.6$, 2.1 Hz, 1H), 7.29 (ddd, $J = 7.1$, 4.9, 1.3 Hz, 1H), 7.80 (ddd, $J = 8.1$, 7.1, 1.5 Hz, 1H), 8.31 (d, $J = 2.2$ Hz, 1H), 8.48 (d, $J = 5.0$ Hz, 1H), 8.55 (d, $J = 8.1$ Hz, 1H), 8.64 ppm (d, $J = 6.4$ Hz, 1H); MALDI-MS: *m*/*z*: 917.9 $[M]^+$.

Synthesis of ruthenium complex 5: A mixture of fulleropyrrolidine **2** (35 mg, 0.038 mmol) and $[Ru(bpy)_2Cl_2]$ (23.3 mg, 0.045 mmol) was refluxed under nitrogen in the dark for 6 h in the presence of excess NH_4PF_6 (61.2 mg, 0.38 mmol) in a mixed solvent DCE (10 mL) and ODCB (10 mL). DCE was removed after the completion of reaction monitored by TLC. Toluene (10 mL) was added to the resulting mixture, and precipitates were collected by means of gravity filtration. The resulting residue was washed with water and toluene four times, until there no color was left in the filtrate, and dried to give products (31.7 mg, 49%). ^{1}H NMR (300 MHz, CD_3CN): $\delta = 2.24$ (s, 4H), 7.30–7.39 (m, 5H), 7.68–7.82 (m. 6H), 8.00–8.11 (m, 6H), 8.42–8.54 ppm (m, 6H); the last four sets of proton peaks were characteristic for ruthenium(II) tris(bipyridine) complexes;[2,3] MALDI-MS: *m*/*z*: 1474.6 $[M-PF_6]^+$, 1328.2 $[M-2PF_6]^+$, 1344.4 $[M-2PF_6+O]^+$, 1360.2 $[M-2PF_6+O_2]^+$.

Synthesis of 4′-hydrazino-2,2′:6′,2″-terpyridine: 4′-Chloro-2,2′:6′,2″-terpyridine (600 mg, 2.2 mmol) was dissolved in isobutanol (12 mL) with warming. Excess of hydrazine (4 mL) was added. The mixture was then heated to reflux under argon, with stirring for overnight. After cooling, white crystals precipitated out of solution. They were collected by filtration and washed with a few drops of water to yield pure 4′-hydrazino-2,2′:6′,2″-terpyridine (489 mg, 84%). M.p 195–197°C; ^{1}H NMR (300 MHz; $CDCl_3$): $\delta = 8.69$ (d, $J = 4.6$ Hz, 2H;), 8.53 (d, $J = 8.0$ Hz, 2H), 7.90 (dd, $J = 7.4$, 1.6 Hz, 2H), 7.82 (s, 2H), 7.41 (dd, $J = 7.4$, 4.9 Hz, 2H), 4.35 (brs, 1H), 3.33 ppm (brs, 2H); MS (ESI): *m*/*z*: 264.26 $[M+H]^+$.

Synthesis of 4′-azido-2,2′:6′,2″-terpyridine: A solution of 4′-hydrazino-2,2′:6′,2″-terpyridine (0.26 g 1.0 mmol) in acetic acid (2.0 mL) and water (1.0 mL) was treated dropwise at 0°C with a cold solution of sodium nitrite (0.69 g; 1.0 mmol) in water (2.0 mL). A pale brown solid was precipitated. When the addition was complete, diethyl ether (20 mL) was added and the aqueous layer was adjusted to alkaline by the addition of solid NaOH beads. The precipitates dissolved and the aqueous phase was further extracted with diethyl ether. The combined organic layers were evaporated and dried to give the product as pale yellow solid (0.27 g, 98%). Crystallization from a mixture of methanol and dichloromethane gave pale yellow needles. ^{1}H NMR (400 MHz $CDCl_3$): $\delta = 7.37$ (ddd, $J =$ 5.9, 4.8, 1.0 Hz, 2H), 7.87 (ddd, $J = 7.8$, 7.4, 1.8 Hz, 2H), 8.16 (s, 2H), 8.60 (d, $J = 8.0$ Hz, 2H), 8.72 ppm (d, $J = 4.7$ Hz, 2H); ^{13}C NMR (100 MHz $CDCl_3$): $\delta = 111.4$, 121.6, 124.3, 137.3, 148.9, 151.0, 155.0, 156.8 ppm; MS (ESI): *m*/*z*: 275 $[M+H]^+$.

Synthesis of 4′-amino-2,2′:6′,2″-terpyridine (6): A solution of 4′-azido-2,2′:6′,2″-terpyridine (0.45 g 1.6 mmol) in a mixture of dichloromethane (5.0 mL) and methanol (5.0 mL) was treated with excess hydrogen sulfide at 0°C, and the solution was kept at room temperature for 5 h until complete consumption of the azido compound. The solution was degassed with nitrogen to remove H_2S and then evaporated to dryness. The residue was treated with 2 M H_2SO_4 and the mixture was filtered and washed with CH_2Cl_2. Subsequently, the remaining solution was basified using 50% NaOH and extracted with CH_2Cl_2. The combined organic layers were evaporated to give pale yellow solid. Crystallization from petroleum ether/dichloromethane gave pale brown solid (0.38 g, 95%). ^{1}H NMR (400 MHz $CDCl_3$): $\delta = 4.35$ (br, 2H), 7.32 (dd, $J = 6.0$, 4.8 Hz, 2H), 7.71 (s, 2H), 7.84 (ddd, $J = 7.7$, 7.4, 1.8 Hz, 2H), 8.59 (d, $J = 8.0$ Hz, 2H), 8.68 ppm (d, $J = 4.7$ Hz, 2H); ^{13}C NMR (100 MHz $CDCl_3$): $\delta = 106.8$, 121.3, 123.6, 136.8, 148.9, 154.6, 156.3, 156.5 ppm; MS: *m*/*z* 248.5 $[M+H]^+$.

Synthesis of *N*-terpyridyl glycine (7): A mixture of 4′-amino-2,2′:6′,2″-terpyridine (0.25 g, 1.2 mmol), ethyl glyoxylate (50% in toluene, 0.24 g, 1.2 mmol), water (1 mL), and concentrated HCl (1 mL) was allowed to stand at 25°C for 1 h in a hydrogenation bottle. Catalyst (100 mg of 10% Pd on carbon) was added, and the mixture was hydrogenated on a low-pressure reaction apparatus charged initially at 35 psi until no further absorption of hydrogen was evident (5 h). Water (3 mL) was added, and the mixture was heated on a water bath to dissolve any white precipitate formed during the reaction. Removal of the catalyst by filtration of the warm mixture and evaporation of the filtrate gave the glycine hydrochloride as white solid. Concentrated HCl was added, and the residue was heated at 60°C for 20 min and then cooled to 0°C. Collection of the solid by vacuum filtration gave (0.18 g, yield 70%) of tan powder in its HCl salt form. The HCl salt was treated with stoichiometric NaOH beads to give compound **7**. ^{1}H NMR (HCl salt; 400 MHz, D_2O): $\delta = 8.58$ (d, $J =$ 5.2 Hz, 2H), 8.35 (t, $J = 7.6$ Hz, 2H), 8.28 (d, $J = 7.8$ Hz, 2H), 7.82 (t, $J =$ 6.4 Hz, 2H), 7.05 (s, 2H), 3.84 ppm (s, 2H); ^{13}C NMR (100 MHz, D_2O): $\delta = 43.6$, 108.6, 123.7, 127.9, 142.2, 145.6, 147.3, 156.5, 172.7 ppm; MS (MALDI): *m*/*z*: 307 $[M+1]^+$, 306 $[M]^+$.

Synthesis of *N*-[4′-(2,2′:6′,2″-terpyridyl)]fulleropyrrolidine (3): A mixture of C_{60} (100 mg, 0.14 mmol), paraformaldehyde (21 mg, 0.7 mmol) and *N*-terpyridylglycine (89 mg, 0.28 mmol) was heated at reflux in *o*-dichlorobenzene (10 mL) under N_2 for 5 h. The reaction mixture was purified by flash column chromatography on silica (eluant: toluene, then toluene/triethylamine 100:6), affording fulleropyrrolidine **3** (46 mg, 48%). ^{1}H NMR (400 MHz, $CDCl_3$): $\delta = 5.53$ (s, 4H), 7.37 (ddd, $J = 6.1$, 4.3, 1.1 Hz, 1H), 7.90 (ddd, $J = 7.9$, 7.1, 1.4 Hz, 1H), 8.43 (s, 2H), 8.71 (d, $J =$ 8.0 Hz, 1H), 8.72 ppm (dd, $J = 5.8$, 1.4 Hz, 2H); ^{13}C NMR (100 MHz, CS_2/$CDCl_3$): $\delta = 61.5$, 69.5, 107.8, 121.4, 123.8, 136.2, 136.5, 140.5, 142.1, 142.2, 142.3, 142.8, 143.3, 144.7, 145.4, 145.7, 145.8, 145.9, 146.2, 146.4, 147.5, 148.9, 154.0, 154.5, 156.3 ppm; MALDI-MS: *m*/*z*: 994.9 $[M]^+$.

Synthesis of ruthenium complex 8: Synthesis of complex **8** followed a similar procedure reported by Diederich and co-workers.[3f] The yield of this reaction was 49%. ^{1}H NMR (500 MHz, CD_2Cl_2): $\delta = 5.79$ (s, 4H), 7.10 (dd, $J = 6.1$, 1.1 Hz, 2H), 7.17 (dd, $J = 5.8$, 1.4 Hz, 2H), 7.26 (dd, $J = 7.9$, 1.4 Hz, 2H), 7.56 (d, $J = 7.5$ Hz, 2H), 7.85 (m, 5H), 8.31 (m, 2H), 8.39 (s, 2H), 8.50 (m, 2H), 8.66 ppm (m, 2H); MALDI-MS: m/z: 1328.7 $[M-2PF_6]^+$, 1473.5 $[M-PF_6]^+$.

Synthesis of $[Ru(tpy)(tpy\text{-}NH_2)][PF_6]_2$ and $[Ru(tpy)_2][PF_6]_2$: Synthesis of the two compounds followed reported procedures.[13]

$[(tpy)Ru(tpy\text{-}NH_2)](PF_6)_2$: ^{1}H NMR (500 MHz, MeOD): $\delta = 7.04$ (ddd, $J = 6.8$, 4.2, 1.3 Hz, 2H), 7.22 (m, 4H), 7.51 (ddd, $J = 7.8$, 7.4, 1.1 Hz, 2H), 7.80 (ddd, $J = 6.5$, 5.3, 1.5 Hz, 2H), 7.88 (ddd, $J = 7.7$, 7.1, 1.0 Hz, 2H), 7.92 (s, 2H), 8.29 (m, 3H), 8.54 (d, $J = 8.0$ Hz, 2H), 8.80 ppm (d, $J = 5.8$ Hz, 2H).

$[Ru(tpy)_2][PF_6]_2$: ^{1}H NMR (500 MHz, MeOD): $\delta = 7.35$ (ddd, $J = 6.7$, 4.2, 1.2 Hz, 4H), 7.73 (dd, $J = 6.0$, 4.8 Hz, 4H), 8.10 (ddd, $J = 7.4$, 7.0, 1.4 Hz, 4H), 8.60 (t, $J = 5.8$ Hz, 2H), 8.82 (d, $J = 8.4$ Hz, 4H), 9.09 ppm (d, $J = 5.9$ Hz, 4H); MALDI-MS: m/z: 567.4 $[M-2PF_6]^+$, 710.5 $[M-PF_6]^+$.

Acknowledgements

Financial support from the National Science Foundation, (Grant No. CHE-0097089 to S.R.W. and D.I.S., CHE-0509989 to L.E. and S.Z.), and the Robert A. Welch Foundation (Grant E-680, K.M.K.) are greatly appreciated. D.M.G. would like to thank the Deutsche Forschungsgemeinschaft, SFB 583, European Commission, FCI, and the Department of Energy for financial support.

[1] a) H. Imahori, Y. Sakata, *Adv. Mater.* **1997**, *9*, 537; b) M. Prato, *J. Mater. Chem.* **1997**, *7*, 1097; c) N. Martin, L. Sanchez, B. Illescas, I. Perez, *Chem. Rev.* **1998**, *98*, 2527; d) H. Imahori, Y. Sakata, *Eur. J. Org. Chem.* **1999**, 2445; e) F. Diederich, M. Gomez-Lopez, *Chem. Soc. Rev.* **1999**, *28*, 263; f) D. M. Guldi, *Chem. Commun.* **2000**, 321; g) C. A. Reed, R. D. Bolskar, *Chem. Rev.* **2000**, *100*, 1075; h) D. Gust, T. A. Moore, A. L. Moore, *J. Photochem. Photobiol. B* **2000**, *58*, 63; i) D. Gust, T. A. Moore, A. L. Moore, *Acc. Chem. Res.* **2001**, *34*, 40; j) D. M. Guldi, N. Martin, *J. Mater. Chem.* **2002**, *12*, 1978; k) D. M. Guldi, *Chem. Soc. Rev.* **2002**, *31*, 22; l) H. Imahori, Y. Mori, Y. Matano, *J. Photochem. Photobiol. C* **2003**, *4*, 51; m) J. F. Nierengarten, *Top. Curr. Chem.* **2003**, *228*, 87; n) D. M. Guldi, *Pure Appl. Chem.* **2003**, *75*, 1069; o) M. E. El-Khouly, O. Ito, F. D'Souza, *J. Photochem. Photobiol. C* **2004**, *5*, 79; p) D. M. Guldi, M. Prato, *Chem. Commun.* **2004**, 2517; q) J. L. Segura, N. Martín, D. M. Guldi, *Chem. Soc. Rev.* **2005**, *34*, 31; r) D. M. Guldi, F. Zerbetto, V. Georgakilas, M. Prato, *Acc. Chem. Res.* **2005**, *38*, 38; s) D. M. Guldi, G. M. A. Rahman, F. Zerbetto, M. Prato, *Acc. Chem. Res.* **2005**, *38*, 871.

[2] a) M. D. Meijer, G. P. M. van Klink, G. van Koten, *Coord. Chem. Rev.* **2002**, *230*, 141; b) *Photochemistry and Photophysics of Coordination Compounds* (Eds: H. Yersin, A. Vogler), Springer, Berlin, **1987**; c) *Photochemistry of Polypyridine and Porphyrin Complexes* (Ed: K. Kalyanasundaram) Academic Press, London, **1991**.

[3] a) F. Cardinali, J. L. Gallani, S. Schergna, M. Maggini, J.-F. Nierengarten, *Tetrahedron Lett.* **2005**, *46*, 2969; b) K. F. Fu, K. Henbest, Y. F. J. Zhang, S. Valentin, Y.-P. Sun, *J. Photochem. Photobiol. A* **2002**, *150*, 143; c) D. M. Guldi, M. Maggini, E. Menna, G. Scorrano, P. Ceroni, M. Marcaccio, F. Paolucci, S. Roffia, *Chem. Eur. J.* **2001**, *7*, 1597; d) D. M. Guldi, M. Maggini, S. Mondini, F. Guerin, J. H. Fendler, *Langmuir* **2000**, *16*, 1311; e) A. Polese, S. Mondini, A. Bianco, C. Toniolo, G. Scorrano, D. M. Guldi, M. Maggini, *J. Am. Chem. Soc.* **1999**, *121*, 3456; f) M. Maggini, D. M. Guldi, S. Simonetta, G. Scorrano, F. Paolucci, P. Ceroni, S. Roffia, *Chem. Eur. J.* **1998**, *4*, 1992; g) D. Armspach, E. C. Constable, F. Diederich, C. E. Housecroft, J.-F. Nierengarten, *Chem. Eur. J.* **1998**, *4*, 723; h) D. Armspach, E. C. Constable, F. Diederich, C. E. Housecroft, J.-F. Nierengarten, *Chem. Commun.* **1996**, 2009; i) M. Maggini, A. Dono, G. Scorrano, M. Prato, *J. Chem. Soc. Chem. Commun.* **1995**, 845; j) N. S. Sariciftci, F. Wudl, A. J. Heeger, M. Maggini, G. Scorrano, M. Prato, J. Bourassa, P. C. Ford, *Chem. Phys. Lett.* **1995**, *247*, 210; k) F. Diederich, C. D. Buchecker, J.-F. Nierengarten, J.-P. Sauvage, *J. Chem. Soc. Chem. Commun.* **1995**, 781; l) F. Chaignon, J. Torroba, E. Blart, M. Borgstrom, L. Hammarstrom, F. Odobel, *New J. Chem.* **2005**, *29*, 1272.

[4] a) *Fullerenes: Chemistry, Physics, and Technology* (Eds.: K. Kadish, R. Ruoff), Wiley, New York, **2000**; b) A. Hirsch, M. Bretreich, *Fullerenes: Chemistry and Reactions*, Wiley-VCH, Weinheim, Germany, **2004**.

[5] a) F. T. Tat, Z. Zhou, S. MacMahon, F. Song, A. Rheingold, L. Echegoyen, S. R. Wilson, *J. Org. Chem.* **2004**, *69*, 4602; b) S. R. Wilson, S. McMahon, F. T. Tat, P. D. Jarowski, D. I. Schuster, *Chem. Commun.* **2003**, 226; c) Z. Ou, Z. Zhou, H. Zhao, F. T. Tat, P. Zhang, S. R. Wilson, K. M. Kadish, *Proc. Electrochem. Soc.* **2004**, *12*, 18.

[6] T. Galili, A. Regev, A. Berg, H. Levanon, D. I. Schuster, K. Möbius, A. Savitsky, *J. Phys. Chem. A* **2005**, *109*, 8451.

[7] J. Modin, H. Johansson, H. Grennberg, *Org. Lett.* **2005**, *7*, 3977.

[8] A. Bagno, S. Claeson, M. Maggini, M. L. Martini, M. Prato, G. Scorrano, *Chem. Eur. J.* **2002**, *8*, 1015.

[9] a) J. M. Tien, I. M. Hunsberger, *J. Am. Chem. Soc.* **1955**, *77*, 6696; b) J. M. Tien, I. M. Hunsberger, *J. Am. Chem. Soc.* **1955**, *77*, 6604.

[10] a) D. Wenkert, and R. B. Woodward, *J. Org. Chem.* **1983**, *48*, 283; b) T. Q. Nguyen, F. Qu, X. Huang, A. F. Janzen, *Can. J. Chem.* **1992**, *70*, 2089; c) M. J. Cook, A. P. Lewis, G. S. G. McAuliffe, V. Skarda, A. J. Thomson, *J. Chem. Soc. Perkin Trans. 2* **1984**, 1293.

[11] G. K. Thomas, V. Biju, M. V. George, D. M. Guldi, P. V. Kamat, *J. Phys. Chem. A* **1998**, *102*, 5341.

[12] a) R. P. Thummel, in *Comprehensive Coordination Chemistry II, Vol. 1* (Ed.: A. P. B. Lever), Elsevier, Amsterdam, **2003**; b) G. Lowe, A. S. Droz, J. J. Park, G. W. Weaver, *Bioorg. Chem.* **1999**, *27*, 477.

[13] S. J. Stoessel, C. M. Elliott, J. K. Stille, *Chem. Mater.* **1989**, *1*, 259.

[14] Z. Zhou, "Tether-Directed Synthetic Approach to Fullerene Multiple Adducts and Investigation of their Metal Binding". Ph.D dissertation, New York University, **2005**.

Received: January 5, 2006
Published online: March 31, 2006

